ISSN : 0974 - 7435 Volume 10 Issue 24

2014

BioTechnology

An Indian Journal

FULL PAPER

BTAIJ, 10(24), 2014 [15894-15904]

Bearingless permanent magnet synchronous motor control using a sliding mode controller with fractional order of suspension forces based on differential geometry

Qiaoqiao Wang[1,2*], Bugong Xu[1], Linru You[1], Xiaohong Wang[1]

[1]College of Automation Science and Engineering South China University of Technology, Guangzhou 510640, (CHINA)

[2]Guangdong Mechanical & Electrical College, Guangzhou 510515, (CHINA)

Email: qqwgd@163.com

ABSTRACT

In this paper, a model of a bearingless permanent magnet synchronous motor is proposed, the expressions of radial suspension forces are derived, and an accurate model is established. Furthermore, decoupling and basic linearization are carried out for the radial suspension forces using the theory of differential geometry, and a sliding mode controller with fractional order based on a neural network is designed for the decoupled, pseudo-linear subsystem. Finally, a simulation experiment is conducted for the designed control system and the feasibility of this decoupling control approach is validated. The simulation results indicate that the application of the proposed control scheme to a bearingless permanent magnet synchronous motor modeled using differential geometry can achieve steady and independent control of radial suspension forces.

KEYWORDS

Bearingless permanent magnet synchronous motor; Differential geometry; Fractional order' Sliding mode control.

© Trade Science Inc.

INTRODUCTION

A bearingless motor is a new type of magnetic suspension motor, whose suspension force is controlled based on the resultant force produced by two kinds of magnets. Because they operate similarly to alternating current motors, in bearingless motors, the suspension control winding which generates the radial force in the magnetic bearing is installed on the motor stator, thus changing the magnetic field distribution in the air gap. Through decoupling control, the motor torque and radial suspension force can be controlled independently, and stable suspension of the motor can be realized. The bearingless permanent magnet synchronous motor (BPMSM) has the advantages of being friction-free, non-abrasive, lubrication- and seal-free, high precision, low maintenance, low cost, etc. Moreover, a magnetizing current is not required. Therefore, BPMSMs are widely used in equipment such as chemical pumps, turbine molecular pumps, blood pumps, high speed milling machines, compression engines, high-speed flywheels, etc.[1].

Due to their nonlinear, multivariate and strong coupling (between the radial suspension forces) features, independent and accurate control for the suspension forces must be realized to enable a basic, stable working condition of a bearingless motor. The sliding mode variable structure control method possesses unique advantages in solving multivariable and nonlinear-coupled problems; hence, this paper applies it to the control of bearingless permanent magnet synchronous motors. Further, nonlinear differential geometry was employed to carry out the decoupling control and linearization of the radial suspension forces. Thus, the original multivariable system was transformed into a non-coupled, pseudo-linear subsystem with two independent radial positions, and then a sliding mode controller with fractional order was designed for the decoupled pseudo-linear subsystem using a neural network. From the simulation results, the feasibility of this kind of decoupling control method was validated, and the control quality and robustness of the system was verified.

THE BASIC PRINCIPLE OF BPMSM AND THE MATHEMATIC MODEL OF THE RADIAL SUSPENSION FORCE

The principle of the rotor radial suspension force produced in a BPMSM can be explained using an equivalent direct-current motor model. Figure 1 shows a schematic diagram describing the radial suspension forces. In a BPMSM, the suspension forces are produced by the combined actions of quadrupole torque windings and dipolar suspension windings, which combined enable stable suspension of the motor. When only the quadrupole torque windings are present, the magnitude of the radial suspension forces is equivalent and the directions of the radial suspension forces are uniformly distributed. So the resultant torque is zero. When the dipolar suspension windings are taken into consideration, the uniform distribution of the magnetic field is broken, and a radial suspension force is produced. Again, consider Figure 1: It can be seen that, according to the given current direction, when the strength of magnetic field in one magnetic pole is weakened, that of the opposite direction will become stronger. So a radial suspension force is produced along the direction of the *x*-axis. If the current in conductor N2 is increased, the radial force will be also increased. However, if the current direction is opposite, the radial force will be produced along the negative *x*-axis. The generation of *y*-axis forces in dipolar windings is similar[2-8].

TPrior to the establishment of our mathematic model, we first hypothesizing assume that the any magnetic circuit saturation of magnetic circuit in the motor is negligible, and the strategy of a rotor orientation strategy is employed in the magnetic suspension system. Furthermore, i_α and i_β are defined as the equivalent currents in the windings N_α and N_β, respectively. Furthermore, $\psi_{\alpha p}$ and $\Psi_{\beta p}$ are defined as the flux linkages produced by the torque equivalent windings of N_α and N_β respectively, L_4 and L_2 are respectively defined as the self-inductances of the torque winding and suspension winding, and $M^{'}$ is defined as the derivative which of the mutual inductance between the torque winding and suspension

winding is relative with respect to the radial displacement of the motor. While Finally, the equivalent currents of suspension windings N*x* and N*y* are defined as i_x and i_y respectively. Then Given the above definitions, the flux linkage of the torque winding in a bearingless permanent magnet synchronous motor BPMSM is: given as

$$\begin{bmatrix} \psi_{\alpha p} \\ \psi_{\beta p} \end{bmatrix} = \begin{bmatrix} L_4 & 0 & M'x & -M'y \\ 0 & L_4 & M'y & M'x \\ M'x & M'y & L_2 & 0 \\ -M'y & M'x & 0 & L_2 \end{bmatrix} \begin{bmatrix} i_\alpha \\ i_\beta \end{bmatrix} \quad \textbf{(1)}$$

in which,

$$M' = \frac{\pi \mu_0 n_4 n_2 l}{8} \frac{r - (l_m + l_g)}{(l_m + l_g)^2} \quad \textbf{(2)}$$

n_4 and n_2 respectively are the HP numbers of the torque winding in the equivalent stator and suspension winding, r is the inner circle radius of the stator, l is the length of the rotor core, μ_0 is the permeability of free space, l_m is the thickness of the permanent magnet, l_g is the thickness of the air gap and $\left(l_m + l_g\right)$ is the length of valid air gap between the stator and rotor.

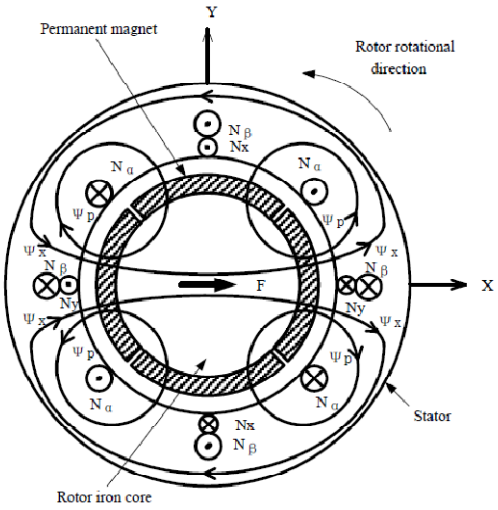

Figure 1: Radial suspension forces generated in a bearingless permanent magnet motor

The magnetic energy stored in the windings can be expressed as

$$W_m = \frac{1}{2} \begin{bmatrix} i_\alpha \\ i_\beta \\ i_x \\ i_y \end{bmatrix}^T \begin{bmatrix} L_4 & 0 & M'x & -M'y \\ 0 & L_4 & M'y & M'x \\ M'x & M'y & L_2 & 0 \\ -M'y & M'x & 0 & L_2 \end{bmatrix} \begin{bmatrix} i_\alpha \\ i_\beta \\ i_x \\ i_y \end{bmatrix} \quad \textbf{(3)}$$

Now, based on the principle of virtual displacement of the electromagnetic field, and ignoring magnetic saturation, the magnetic suspension forces fed by eccentric shafts in x and y can be represented as：

$$\begin{bmatrix} F_x \\ F_y \end{bmatrix} = \begin{bmatrix} \frac{\partial W_m}{\partial x} \\ \frac{\partial W_m}{\partial y} \end{bmatrix} \tag{4}$$

Substituting Eqs (1), (2) and (3) into Eq (4) results in

$$\begin{bmatrix} F_x \\ F_y \end{bmatrix} = \begin{bmatrix} M i_\alpha & M i_\beta \\ -M i_\beta & M i_\alpha \end{bmatrix} \begin{bmatrix} i_x \\ i_y \end{bmatrix} \tag{5}$$

The radial suspension force, which is produced by the uneven distribution of the air-gap field caused by the eccentricity of stator and rotor, can be expressed as

$$\begin{cases} f_x = k_s x \\ f_y = k_s y \end{cases} \tag{6}$$

where k_s is the stiffness of radial displacement.

The equation of rotor motion for a BPMSM is then given by Newton's second law as

$$\begin{cases} F_x - f_x = m\ddot{x} \\ F_y - f_y = m\ddot{y} \end{cases} \tag{7}$$

where m is the mass of the rotor.

According to Eq (7), the mathematical model of the radial suspension force in a rotor during eccentricity can then be expressed as

$$\begin{cases} \ddot{x} = \dfrac{M}{m}\left(i_\alpha i_x + i_\beta i_y\right) + \dfrac{1}{m} k_s x \\ \ddot{y} = \dfrac{M}{m}\left(-i_\beta i_x + i_\alpha i_y\right) + \dfrac{1}{m} k_s y \end{cases} \tag{8}$$

It can be seen from Eq (8) that when the motor operates in a condition of constant load, the current component of the torque is also a constant value, and further, the radial force and the current of the suspension winding are nonlinearly coupled.

To further characterize the system, state variable vector $X = \begin{bmatrix} x_1 & x_2 & x_3 & x_4 \end{bmatrix}^T = \begin{bmatrix} x & y & \dot{x} & \dot{y} \end{bmatrix}^T$, input variables $U = \begin{bmatrix} u_1 & u_2 \end{bmatrix}^T = \begin{bmatrix} i_x & i_y \end{bmatrix}^T$ and output variables $Y = \begin{bmatrix} y_1 & y_2 \end{bmatrix}^T = \begin{bmatrix} x & y \end{bmatrix}^T$ are selected so as to obtain the state equation

$$\begin{cases} X = f(X) + \sum_{i=1}^{2} g_i(X) u_i \\ y_1 = h_1(X) \\ y_2 = h_2(X) \end{cases} \tag{9}$$

$$f(X)=\begin{bmatrix} x_3 & x_4 & k_s/m\,x_1 & k_s/m\,x2 \end{bmatrix}^T,$$

$$g_1(X)=\begin{bmatrix} 0 & 0 & M'/m\,i_\alpha & -M'/m\,i_\beta \end{bmatrix}^T,$$

$$g_2(X)=\begin{bmatrix} 0 & 0 & M'/m\,i_\beta & M'/m\,i_\alpha \end{bmatrix}^T.$$

The system is a typical affine, nonlinear system defined in a four dimensional space with continuity C^∞ and popular $M=\left\{X=\begin{bmatrix} x_1 & x_2 & x_3 & x_4 \end{bmatrix}^T\right\}$.

THE LINEAR DECOUPLING OF RADIAL SUSPENSION FORCE FOR BPMSM BASED ON DIFFERENTIAL GEOMETRY

For the given multivariable nonlinear system

$$\begin{cases} X=f(X)+\sum_{i=1}^{2} g_i(X)u_i \\ y_j=h_j(X), j=1\cdots m \end{cases} \tag{10}$$

in which X is defined as the local coordinates of popular M in an n-dimensional space with continuity C^∞, $f, g_1, g_2, \cdots, g_l$ are vector fields of C^∞ in M, and h is a mapping of C^∞ in M, that is $h: M^{\rightarrow} R^j$; y is the output.

Next, we define

$$D(X)=\begin{bmatrix} L_{g1}L_f^{r_1-1}h_1(X),\cdots L_{gl}L_f^{r_m-1}h_1(X) \\ \cdots\cdots\cdots\cdots\cdots\cdots \\ L_{g1}L_f^{r_1-1}h_m(X),\cdots L_{gl}L_f^{r_m-1}h_m(X) \end{bmatrix},\ E(X)=\begin{bmatrix} L_f^{r_1}h_1(X) \\ \vdots \\ \vdots \\ L_f^{r_m}h_m(X) \end{bmatrix}.$$

The sufficient and necessary condition for decoupling of the nonlinear system is that matrix $D(X)$ is nonsingular on M[12]. The state feedback control law is given by

$$u=\alpha(x)+\beta(X)v=-\left[D(X)\right]^{-1}E(X)+\left[D(X)\right]^{-1}v \tag{11}$$

The system can then be decoupled in M as

$$\begin{cases} \dot{X}=f(X)+g(X)\alpha(X)+g(X)\beta(X)v \\ y_j=h_j(X), j=1,2,\cdots,m \end{cases} \tag{12}$$

where the output functions are $h_1(X)=x_1, h_2(X)=x_2$. Next, we define

$L_f h_1(X) = x_3$

$L_f h_2(X) = x_3$

$L_g h_1(X) = (0 \quad 0)^{'}$

$L_g h_2(X) = (0 \quad 0)$

Giving

$$L_g L_f h_1(X) = \left[M^{'}/_m i_\alpha \quad M^{'}/_m i_\beta \right] \tag{13}$$

$$L_g L_f h_2(X) = \left[-M^{'}/_m i_\beta \quad M^{'}/_m i_\alpha \right] \tag{14}$$

From Eqs (13) and (14), we find that $r_i = r_2 = 2$, and

$$D(X) = \begin{bmatrix} L_{g1} L_f^{r_1 - 1} h_1(X), \cdots L_{gl} L_f^{r_m - 1} h_1(X) \\ \cdots\cdots\cdots\cdots\cdots\cdots \\ L_{g1} L_f^{r_1 - 1} h_m(X), \cdots L_{gl} L_f^{r_m - 1} h_m(X) \end{bmatrix} =$$

$$\begin{bmatrix} M^{'}/_m i_\alpha & M^{'}/_m i_\beta \\ -M^{'}/_m i_\beta & M^{'}/_m i_\alpha \end{bmatrix}$$

$$E(X) = \begin{bmatrix} L_f^{r_1} h_1(X) \\ \vdots \\ \vdots \\ L_f^{r_m} h_m(X) \end{bmatrix} = \begin{bmatrix} k_s/_m x_1 \\ k_s/_m x_2 \end{bmatrix}.$$

Finally, we have that

$$\lim_{x \to 0} \det\left[D(X) \right] = \left(M^{'}/_m i_\alpha \right)^2 + \left(M^{'}/_m i_\beta \right)^2 \neq 0,$$

so that $D(X)$ is nonsingular and meets the decoupling condition.

For Eq (12), since $\sum_{i=1}^{2} r_i = 4 = n$, the new coordinates can be obtained from the transformation of $z = \varphi(x)$ as

$$\begin{cases} z_1^0 = \varphi_1(X) = h_1(X) = x_1 \\ z_1^1 = \varphi_2(X) = L_f h_1(X) = x_3 \\ z_2^0 = \varphi_3(X) = h_2(X) = x_2 \\ z_2^1 = \varphi_4(X) = L_f h_2(X) = x_4 \\ y_1 = h_1(X) = z_1^0 \\ y_2 = h_2(X) = z_2^0 \end{cases} \tag{15}$$

The state function of the system under the new coordinate system is given by

$$\begin{cases}\begin{bmatrix}\dot{z}_1^0\\ \dot{z}_1^1\end{bmatrix}=\begin{bmatrix}0 & 1\\ 0 & 0\end{bmatrix}\begin{bmatrix}z_1^0\\ z_1^1\end{bmatrix}+\begin{bmatrix}0\\ 1\end{bmatrix}v_1; y_1=\begin{bmatrix}1 & 0\end{bmatrix}\begin{bmatrix}z_1^0\\ z_1^1\end{bmatrix}\\ \begin{bmatrix}\dot{z}_2^0\\ \dot{z}_2^1\end{bmatrix}=\begin{bmatrix}0 & 1\\ 0 & 0\end{bmatrix}\begin{bmatrix}z_2^0\\ z_2^1\end{bmatrix}+\begin{bmatrix}0\\ 1\end{bmatrix}v_2; y_2=\begin{bmatrix}1 & 0\end{bmatrix}\begin{bmatrix}z_2^0\\ z_2^1\end{bmatrix}\end{cases} \quad (16)$$

Finally, it is evident that the original system can be decoupled into two independent subsystems, and each of them is in the linear controllable canonical form with critical stability.

DESIGN OF A SLIDING MODE CONTROLLER WITH FRACTIONAL ORDER BASED ON A NEURAL NETWORK

A sliding mode controller with fractional order based on a neural network can be designed for the two decoupled pseudo-linear subsystems described above. A sliding mode controller is a robust method for nonlinear control. It can purposefully and continuously change the structure of the controller according to the current state of system (e.g. deviation, order, etc.) and the chosen switching manifold, which forces it to move along a predetermined state trajectory. Once the state trajectory of the system enters a sliding mode state, the system will be completely self-adaptive and invariable to interference and any variation of its parameters. However, in practical applications, the following three facts, 1) the output of a sliding mode controller consists of oppositely signed switching parameters at high frequency, 2) the switching device of the actual system has inertia, 3) and the BPMSM is a time-varying system with strong coupling and load disturbance, may result in the actual state of the sliding mode not occurring in the setting switch manifold, which easily causes high frequency chattering of the system. This chattering phenomenon limits the application of the nonlinear control method—the sliding mode variable structure—in some circumstances requiring high accuracy[15].

Specific to the chattering problem in sliding mode control systems, the theory of fractional calculus is introduced into sliding mode control in this paper. By using the strong learning ability of neural networks, a control system is designed based on the surface of sliding mode with fractional order so that the controller can achieve robust control of an uncertain system and eliminate the chattering phenomenon. The control block scheme of the sliding mode control system with fractional order based on a neural network is shown in Figure 2. The design of the controller includes two parts: The design of the switching surface and the learning algorithm of the network weights.

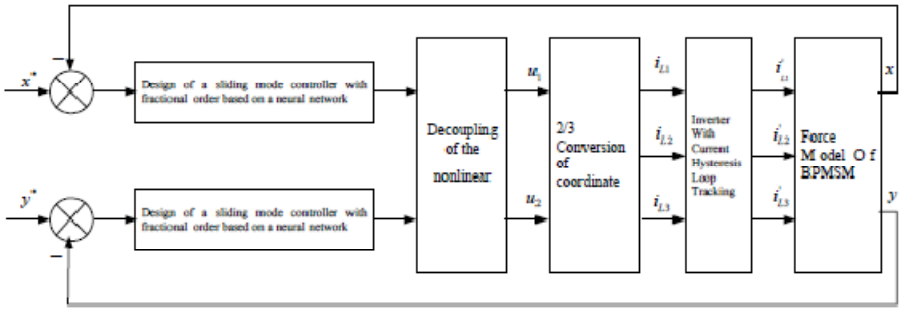

Figure 2: A block diagram of the control system

Considering the controlled object as:

$$\begin{cases}\dot{x}=x_2\\ \dot{x}_2=f(x)+bu+d(t)\end{cases} \quad (17)$$

and defining the position as *r*, system error as *e*, and the velocity error of *e* as

$$\begin{cases} e(t) = r(t) - x_1 \\ \dot{e}(t) = \dot{r}(t) - x_1 \end{cases} \tag{18}$$

the switching function of fractional order is then

$$s = cx + {}_0D_t^{(1-r)}x \tag{19}$$

where $c \in R^+$, and the selection of c directly determines the dynamic quality of the sliding mode control for system.

The output of the neural sliding mode controller is given as

$$u = \sum_{j=1}^{m} \omega_j h_j = \sum_{j=1}^{m} \omega_j \exp\left(-\frac{\left\| s - c_j \right\|^2}{b_j} \right) \tag{20}$$

where $h_j = \exp\left(-\frac{\left\| s - c_j \right\|^2}{b_j} \right)$ is a Gaussian function, ω_j is the weight vector of the network, c_j is the central vector of the node j, b_j is the base width for network node j and m is the neuron number of the implicit layer. The outputs of the neural sliding mode control system must assure the system state meets the condition $s(t)\dot{s}(t) \le o$. The following performance indexes of control are taken into consideration:

$$E = s(t)\,{}_0D_t^r s(t) \tag{21}$$

where ${}_0D_t^r(\cdot)$ is the fractional derivative, 0 and t are the upper and lower limits of integration and r is the order. The definition of the fractional order derivative is[16]

$${}_0D_t^r f(t) = \begin{cases} \frac{1}{\Gamma(n-r)} \int_0^t \frac{f^{(n)}(\tau)}{(t-\tau)^{r+1-n}} d\tau, & n-1 < r < n \\ \frac{d^n}{dt^n} f(t), & r = n \end{cases} \tag{22}$$

Based on Eq (22), when n=1, we have

$$s\,{}_0D_t^r s = s \frac{1}{\Gamma(1-r)} \int_0^t \frac{\dot{s}}{(t-\tau)^r} d\tau, \tag{23}$$

Only if the following condition is satisfied can the output of the neural sliding mode control system assure that the system state meets the constraint $s(t)\dot{s}(t) \le o$,

$$E = s(t)\,{}_0D_t^r s(t) \le 0 \tag{24}$$

The following learning algorithm of network weights is adopted:

$$w_j(k) = w_j(k-1) + \eta \Delta w_j(k) + \alpha\left(w_j(k-1) - w_j(k-2)\right) \quad \textbf{(25)}$$

$$\Delta w_j(k) = \frac{\partial E(k)}{\partial w_j} = -{}_0D_t^r s(k) \frac{\partial {}_0D_t^r s(k)}{\partial u(k)} \frac{\partial u(k)}{\partial w_j} = -{}_0D_t^r s(k) B h_j$$

in which, η is the learning rate, and α is a momentum factor.

SIMULATION EXPERIMENT

In order to validate the control strategy for the pseudo-linear subsystem derived from the decoupling and linearization, the Matlab toolbox Simulink is adopted to construct the control system simulation. During the simulation process, the parameters of the neural sliding mode variable structure are initialized as random values. The parameters of the Gaussian function are $c = \begin{bmatrix} -2 & -1.5 & 0 & 1.55 \end{bmatrix}$ and $b = \begin{bmatrix} 1 & 1 & 1 & 1 \end{bmatrix}^T$. The parameters of motor were given as: The mass of rotor was m=0.5 kg, the moment of inertia was J=3.9x10^{-4}kgm^2, the number of pole-pairs in torque winding is $P = 1$, the stator resistance is 2Ω, $M^{'}$=3.8 mH and the linkage of the permanent magnet pole and stator winding is 0.125 Wb. The given rotational speed is 800 rad/s. In the simulation experiment, with the initial eccentric displacement of rotor centroid given as $x_0 = 0mm, y_0 = -0.025mm$, the response curve in the *y*-direction is shown in Figure 3.

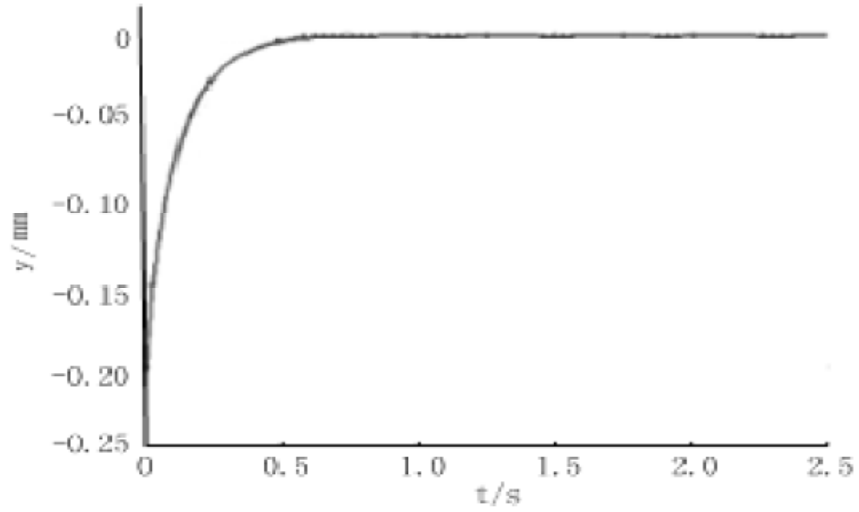

Figure 3: The response curve of the displacement in the *y*-direction

It can be seen from Figure 3 that the rotor comes into stable suspension very quickly. In order to further understand the disturbance resisting capabilities of our scheme, 300 N external disturbing forces in f_x and f_y are applied to the rotor in t=0.7 and t=1.9. In the simulation, the rotors are subjected to the disturbances and fluctuation of displacement is apparent; however, the rotor can be still stably suspended as shown in Figure 4.

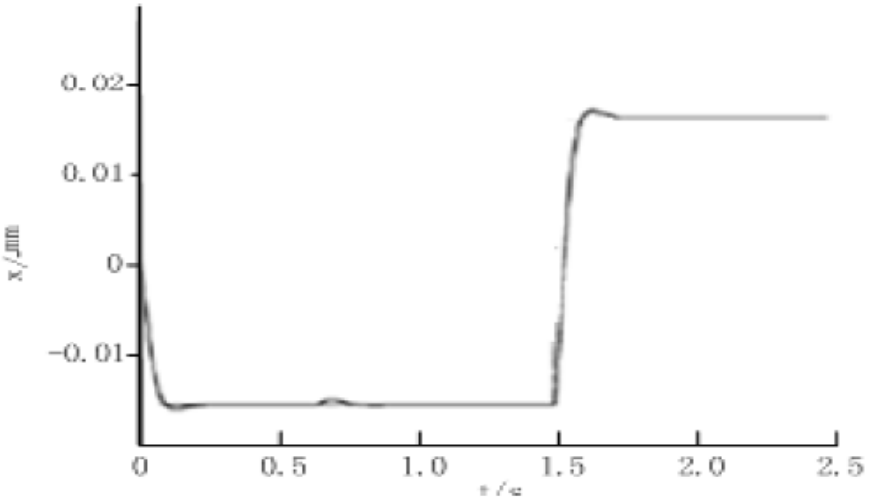

(a) The radial displacement in the *x*-axis

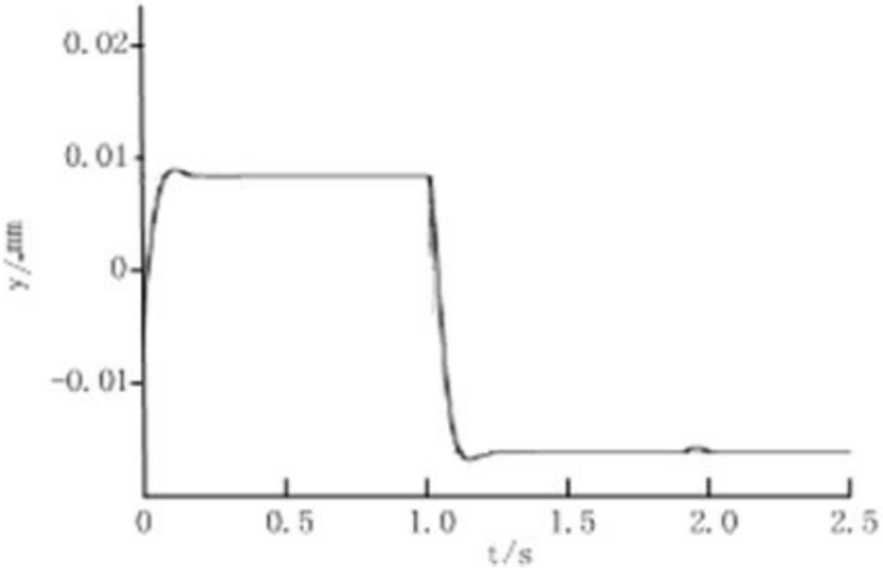

(b) The radial displacement in the *y*-axis

Figure 4: Response curves of the radial displacements with an applied disturbance

CONCLUSIONS

Using basic principles of the operation of bearingless permanent magnet synchronous motors, this paper developed a mathematic model of the radial suspension forces for a BPMSM. Nonlinear differential geometry was employed to conduct the basic linearization of the radial suspension forces. A sliding mode controller with fractional order based on a neural network was designed for the decoupled pseudo-linear subsystem resulting from the above analysis and a simulation was implemented and tested. The results of the simulation show that our control scheme has desirable static and dynamic performance and strong robustness, which establishes a foundation for further research on the radial suspension forces of bearingless motors, decoupling control of electromagnetic torque and the motor with various loads.

REFERENCES

[1] Akira Chiba, Tadashi Fukao, Osamu Ichikawa, Masahide Oshima, Masatugu Takemoto, David Dorrell;

Magnetic Bearings and Bearingless Drives, Newnes, UK Mar **(2005)**.

[2] L.Hertel, W.Hofmann; "Theory and Test Results of a High Speed Bearingless Reluctance Motor", PCIM, Nuremberg, Germany, 143-147 **(1999)**.

[3] Masahide Ooshima; "Analyses of Rotational Torque and Suspension Force in a Permanent Magnet Synchronous Bearingless Motor with Short-pitch Winding", IEEE Power Engineering Society 2007 General Meeting, Tampa, Florida, USA, 1-7 Jun **(2007)**.

[4] Xiaoting Ye, Jie Tang, Tao Zhang; "Research for the Design Scheme of Bearingless Motors", International Conference on Electrical Machines and Systems, wuhan, China, 208-211 Oct **(2008)**.

[5] A.Chiba, T.Deido, T.Fukao, M.A.Rahman; "An analysis of bearingless AC motors",IEEE Transactions on Energy Conversion, **9(1)**, 61-68 Mar **(1994)**.

[6] M.Ooshima, S.Miyazawa, T.Deido, A.Chiba, F.Nakamura, T.Fukao; "Characteristics of a Permanent Magnet Type Bearingless Motor", IEEE Transactions on Industry Applications, **32(2)**, 363-370 **(1996)**.

[7] M.Ooshima, A.Chiba, T.Fukao, M.A.Rahman; "Design and Analysis of Permanent Magnet-Type Bearingless Motors", IEEE Transactions on Industrial Electronics, **43(2)**, 292-299 **(1996)**.

[8] M.Ooshima, S.Miyazawa, A.Chiba, F.Nakamura, T.Fukao; "Performance Evaluation and Test Results of a 11 000 r/min, 4 kW Surface-Mounted Permanent Magnet-Type Bearingless Motor", Proc. of 7th Int. Symposium on Magnetic Bearings, 377-382 **(2000)**.

[9] Zhu Huang-qiu, Hao Xiao-hong, Zhang Ting-ting, Diao Xiao-yan; Neural SMVS Decoupling Control of BearinglessMotor Based on Differential Geometry [J], Control Engineering of China, **18(1)**, 9-13 **(2011)**.

[10] D.Wang, B.Chen, P.Ju; Study on mechanism of bearingless permanent magnet-type motors to produce radial suspension force [J], Journal of Jiangsu University (Natural Science Edition), **25(5)**, 434-437 **(2004)**.

[11] Y.Okada, S.Shimura, T.Ohishi; "Horizontal Experiments on a Permanent Magnet Synchronous Type and Induction Type Levitated Rotating Motor", Proc. of IPEC-Yokohama, 340-345 **(1995)**.

[12] Hu Yue ming; Nonlinear control theory and application [M], National Defence of Industry Press, Bejing, **(2002)**.

[13] Liu Jinkun; Sliding mode variable structure control using Matlab simulation[M], Beijing: Tsinghua University Press **(2005)**.

[14] K.Nenninger, W.Amrhein, S.Silber, G.Trauner, M.Reisinger; "Magnetic Circuit Design of a Bearingless Single-Phase Slice Motor", Proc. of 8th Int. Symposium on Magnetic Bearings, 265-270 **(2002)**.

[15] Zhang BiTao; Research for intelligent fractional order sliding mode control and system parameters tuning, Doctor Dissertation, 06 **(2012)**.

[16] I.Podlubny; Fractional Differential Equations, Academic Press, NewYork **(1999)**.